COMMUNICATION

ChemComm
www.rsc.org/chemcomm

Preparation of highly dispersed RhPt alloy catalysts in mesoporous silica using supercritical carbon dioxide and selective synthesis of ethane in butane hydrogenolysis†

Paresh L. Dhepe,[b] Atsushi Fukuoka*[ab] and Masaru Ichikawa*[ab]

[a] *Catalysis Research Center, Hokkaido University, Sapporo 060-0811, Japan*

[b] *Division of Chemistry, Graduate School of Science, Hokkaido University, Sapporo 060-0810, Japan. E-mail: fukuoka@cat.hokudai.ac.jp, michi@cat.hokudai.ac.jp*

Received (in Cambridge, UK) 27th November 2002, Accepted 15th January 2003
First published as an Advance Article on the web 30th January 2003

RhPt alloy catalysts were prepared in mesoporous silica using supercritical carbon dioxide in impregnation to achieve high dispersion with controlled morphology; catalytic activity and ethane selectivity are enhanced in butane hydrogenolysis.

Preparation of highly dispersed metal particles on supports is of great interest to improve catalytic activity and selectivity of heterogeneous catalysts.[1,2] With controlled composition, highly dispersed bimetallic particles are attracting much attention, since they show very different properties compared to monometallic catalysts.[3] From an environmental point of view, use of organic solvents needs to be reduced and nowadays research has been concentrating on the utilization of environmentally benign solvents like supercritical fluids (SCF). Supercritical carbon dioxide ($scCO_2$) is a cheap, non-toxic and non-flammable source that is widely used as a reaction media.[4,5] On the other hand, $scCO_2$ is used in the synthesis of nanoporous materials by a nanocasting process.[6] The advantages of supercritical fluids are alterable gas–liquid properties, high diffusivity over gases and low viscosity over liquids. We demonstrated benefit of $scCO_2$ in achieving highly dispersed Rh nanoparticles in mesoporous silica FSM-16.[7] It is expected that the use of SCF would be beneficial in the synthesis of bimetallic particles with controlled size and composition. By far SCF has not been applied to the preparation of bimetallic catalysts. In this communication we report preparation of SiO_2 and FSM-16 supported bimetallic RhPt catalyst using $scCO_2$. The catalysts show higher dispersion and homogeneous alloy formation after $scCO_2$ treatment over conventional catalysts.

Mesoporous silica FSM-16 has a similar structure as that for MCM-41 with highly ordered hexagonal array of one-dimensional channels with pore diameter 2.7 nm.[8] RhPt catalysts were prepared by the impregnation method and were treated with $scCO_2$.‡ Characterization was done by CO chemisorption, XRD, TEM and IR. Butane hydrogenolysis was performed as a test reaction in a fixed-bed flow reactor at atmospheric pressure.

CO uptake indicated the formation of highly dispersed bimetallic nanoparticles on FSM-16 after the $scCO_2$ treatment [Table 1]. The $scCO_2$-treated RhPt/FSM-16 catalysts showed higher metal dispersions over non-treated catalysts (91 over 67%) [entries 1 and 2]. SiO_2-supported RhPt catalyst was prepared under similar conditions, where dispersion was restricted at 36% [entries 3 and 4] probably because of low surface area of SiO_2 (300 $m^2\ g^{-1}$) compared to FSM-16 (980 $m^2\ g^{-1}$). The $scCO_2$-treated Rh catalysts also have higher metal dispersion over non-treated catalysts [entries 5–8].

The low angle XRD pattern (2θ = 1.5–10°) confirmed that 2D-hexagonal structure (*P*6mm) was preserved after the $scCO_2$-treatment. The high angle XRD pattern (2θ = 30–90°) showed an *fcc* metal crystal phase (ESI, Fig. S1 and S2†).

The mean particle size calculated from the TEM image was 2.5 nm for the $scCO_2$-treated catalyst. This shows the formation of metal particles inside the mesoporous channels (diameter 2.7 nm) of FSM-16 [Fig. 1a]. It points out that high diffusivity of $scCO_2$ carries metal precursors inside the channels. For the non-treated catalysts, the mean particle size was 5 nm indicating the formation of particles on the external surface of the support [Fig. 1b].

In the IR spectroscopy of the CO adsorption on RhPt/FSM-16, peak pattern was totally different for the non-treated and the $scCO_2$-treated catalysts [Fig. 2].§ Deconvolution of the spectrum was done using the GRAM Al32 program (Galactic), and in the case of the non-treated catalyst [Fig. 2b], peaks at 2108 and 2038 cm^{-1} corresponding to geminal dicarbonyl species $[Rh(CO)_2]^+$ were observed.[9] Similarly another pair for the geminal dicarbonyl species were observed at 2094 and 2027 cm^{-1}. Formation of two set of $[Rh(CO)_2]^+$ species is explained by the slight difference in oxide ligands except for CO.[10] The 2068 cm^{-1} peak can be ascribed to Rh^0-CO since Pt/FSM-16 at the same loading (Pt 0.75 wt%) gave only small peaks. The $scCO_2$-treated catalysts showed a major peak at the same frequency (2067 cm^{-1}) corresponding to Rh^0-CO [Fig. 2a].[11] Moreover the 2045 cm^{-1} peak is assignable to another Rh^0-CO

† Electronic supplementary information (ESI) available: Figs. S1 and S2, Schemes S1 and S2. See http://www.rsc.org/suppdata/cc/b2/b211680d/

Table 1 Results of hydrogenolysis of butane by supported RhPt and Rh catalysts[a]

Entry	Catalyst	Treat[b]	CO/M[c]	Mean particle size by TEM/ nm	n-butane conversion/%	Product distibution (%)[d]			
						CH_4	C_2H_6	C_3H_8	C2/C3
1	RhPt/FSM-16	$scCO_2$	0.91	2.5	71	7	86	6	14.3
2	RhPt/FSM-16	Non-treat	0.67	5.0	46	11	79	10	7.9
3	RhPt/SiO_2	$scCO_2$	0.36	n.d.	7	16	68	16	4.2
4	RhPt/SiO_2	Non-treat	0.36	n.d.	4	9	82	9	9.1
5	Rh/FSM-16	$scCO_2$	0.67	2.0	39	8	84	7	12.0
6	Rh/FSM-16	Non-treat	n. d.	4.0	25	16	69	14	4.9
7	Rh/SiO_2	$scCO_2$	0.22	n.d.	5	35	31	34	0.9
8	Rh/SiO_2	Non-treat	0.16	n.d.	2	29	45	26	1.1

[a] Reaction conditions: Catalyst, 0.15 g, 20–42 mesh. Gas flow H_2:n-C_4H_{10} = 9:1. Total pressure 133 kPa. GHSV = 3800 h^{-1}. Temperature, 453 K. The data were taken after 4 h of reaction time. [b] $scCO_2$, supercritical CO_2 treatment. [c] CO uptake at 323 K in the pulse mode. [d] Product distribution is calculated as mole percentage of products.

DOI: 10.1039/b211680d

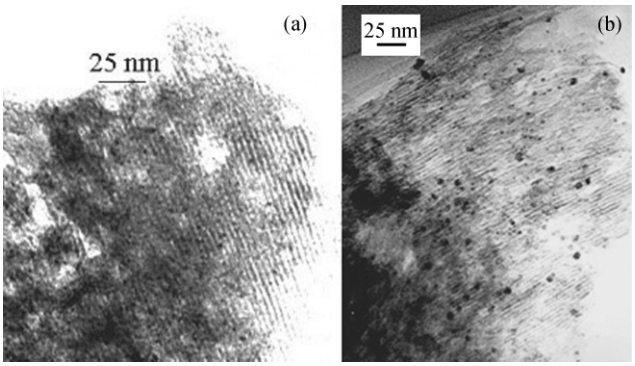

Fig. 1 TEM images of RhPt/FSM-16 catalysts, (a) $scCO_2$ treated and (b) non-treated.

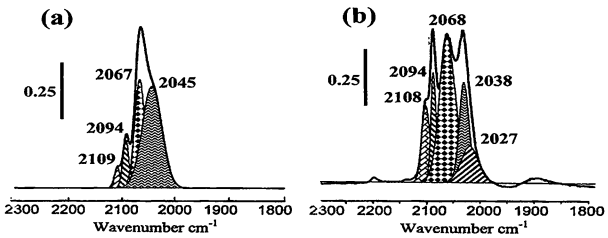

Fig. 2 IR spectra for CO adsorption on RhPt/FSM-16 catalysts, (a) $scCO_2$ treated and (b) non-treated.

species.[9] The contribution of $[Rh(CO)_2]^+$ species is low, and their counterparts are masked in the 2045 cm^{-1} broad peak. The formation of $[Rh(CO)_2]^+$ on the oxide surface is explained by oxidation of Rh by the surface OH groups.[11,12] First, mobile metal carbonyl species (Rh-CO) are formed after CO adsorption, and these species diffuse across the surface and become stabilised by interaction with the surface OH groups to form dicarbonyl species.[11,12] The mobility and interaction with surface OH groups of Rh-CO species are strongly influenced by the nature of the support surface. Nieuwenhuys reported that Pt may restrict Rh to form geminal dicarbonyl species if Rh and Pt are in the close vicinity of each other on SiO_2, giving rise to only Rh^0-CO species.[13] In our $scCO_2$-treated catalysts we observed major peaks for Rh^0-CO species which are due to the presence of Pt that modifies Rh ensembles, leading to lower mobility of Rh-CO species. This causes weaker interaction of Rh with surface OH groups to restrict the formation of $[Rh(CO)_2]^+$. Therefore we argue that after the $scCO_2$ treatment, Rh and Pt form homogenous alloys and not alike non-treated catalysts where we observed peaks due to dicarbonyl species because of separate Rh and Pt particle formation.

The characterization results indicate formation of highly dispersed bimetallic alloy particles after the $scCO_2$ treatment. It is plausible that metal precursors dissolved under supercritical conditions can be homogeneously distributed across the support surface because of high diffusivity of $scCO_2$ compared to organic solvents, which helps to place precursors inside the channels. Gas-like properties of $scCO_2$ suppress the aggregation of metal precursor on the external surface, which is frequently observed for conventional organic solvents due to capillary action force generated during the drying process.

The results of butane hydrogenolysis are summarized in Table 1. Under the conditions of 453 K and 133 kPa, Pt/FSM-16 is completely inactive towards C–C bond cleavage so that the catalytic activity is only due to Rh in bimetallic catalysts. The $scCO_2$-treated RhPt/FSM-16 catalyst showed highest conversion (71%) [entry 1] and gave improved activity over the non-treated catalyst (46%) [entry 2]. This also corresponds to a 10% increase of turnover frequency based on surface atoms. FSM-16 is a better support than silica. Difference in the activity may arise from particle size or effect of channel structure of FSM-16. The $scCO_2$-treated silica and FSM-16 supported monometallic Rh catalysts also have higher activities over non-treated catalysts [entries 5–8].

The selectivity pattern was affected by the $scCO_2$ treatment and Pt. It is reported that the ethane selectivity increases as the particle size decreases.[14] Notably the $scCO_2$-treated RhPt/FSM-16 showed high selectivity to ethane (86%) [entry 1]. Typical product distribution (C1:C2:C3 = 1:2:1) was observed for the Rh/SiO_2 (non-treated) catalyst [entry 8]. For FSM-16 supported $scCO_2$-treated and non-treated catalysts, a higher ethane selectivity was obtained at 453 K as shown in entries 1, 2, 5 and 6. However, monometallic Rh/FSM-16 showed 100% conversion at 493 K with multiple hydrogenolysis of ethane and propane to methane (C1: 50%, C2: 48%, C3: 2%). On the contrary, over RhPt/FSM-16 at 473 K multiple hydrogenolysis was markedly suppressed at 100% conversion to give ethane as a main product (C1: 14%, C2: 82%, C3: 4%).

It has been proposed that the hydrogenolysis proceeds *via* adsorbed hydrocarbon species formed by loss of one or more hydrogen atom(s) followed by C–C bond cleavage and further attack by hydrogen.[15] We propose that active Rh ensembles divided by Pt yield ethane by central C–C bond cleavage through 1,2-adsorption rather than 1,3-adsorption of butane (ESI, Scheme S1 and S2†). Because Pt is known to activate and spill over H_2 even at room temperature, we suggest that Pt promotes the 1,2-adsorption of n-butane on Rh and the successive hydrogenation to form ethane as a main product.

In conclusion, $scCO_2$ treatment during catalyst preparation is a very promising pathway to achieve the desired morphology of the highly dispersed metal particles due to the higher diffusing power of $scCO_2$ over conventional organic solvents. Catalytic performances and ethane selectivity of the $scCO_2$-treated catalysts were improved over non-treated, conventional catalysts.

We thank Toyota R & D Labs., Inc. for generous donation of FSM-16 and Fuji Silysia for CARiACT silica support. This work was supported by a Grant-in-Aid for Scientific Research from the Ministry of Education, Science, Sports and Culture, Japan (No. 13650836).

Notes and references

‡ Bimetallic catalysts were prepared by dissolving $[Rh(OAc)_2]_2$ and $Pt(acac)_2$ in THF and impregnated on FSM-16 (BET: 980 $m^2\ g^{-1}$, pore diameter: 2.7 nm) or SiO_2 (CARiACT, Q10, 300 $m^2\ g^{-1}$)(Pt:Rh = 0.2 atomic ratio, Rh 2 wt%, Pt 0.75 wt%). THF was removed under vacuum and then the powder sample was divided into two parts: one part was given the $scCO_2$-treatment at 348 K and 20 MPa for 24 h under stirring. The other part was not treated with $scCO_2$. Then the powders were calcined under air and reduced in H_2 flow for 2 h at 673 K each. Monometallic SiO_2 and FSM-16 supported Rh (2.5 wt%) and FSM-16 supported Pt (0.75 wt%) catalysts were prepared by a similar preparation method.

§ For the IR of CO, a self-supported wafer (~20 mg) was reduced under H_2 (26.6 kPa) at 473 K for 1 h followed by evacuation for 30 min. After cooling down to room temperature, CO (26.6 kPa) was admitted for 1 h. The cell was evacuated and spectra were measured at a resolution of 2 cm^{-1} with 100 interferrograms.

1 B. C. Gates, *Catalytic Chemistry,* Wiley, New York, 1992.
2 M. Ichikawa, *Adv. Catal*., 1992, **38**, 283.
3 J. H. Sinfelt, *Bimetallic Catalysts,* Wiley, New York, 1983.
4 P. G. Jessop, T. Ikariya and R. Noyori, *Chem. Rev*., 1999, **99**, 475.
5 A. Baiker, *Chem. Rev*., 1999, **99**, 453.
6 H. Wakayama and Y. Fukushima, *Chem. Commun*., 1999, **4**, 391.
7 P. L. Dhepe, A. Fukuoka and M. Ichikawa, *Catal. Lett*., 2002, **81**, 69.
8 S. Inagaki, Y. Fukushima and K. Kuroda, *J. Chem. Soc., Chem. Commun*., 1993, **8**, 680.
9 A. C. Yang and C. W. Garland, *J. Phys. Chem*., 1957, **61**, 1504.
10 R. D. Shannon, J. C. Vedrine, C. Naccache and F. Lefebvre, *J. Catal*., 1984, **88**, 431.
11 J. A. Anderson and F. Solymosi, *J. Chem. Soc., Faraday Trans*., 1991, **87**, 3435.
12 A. K. Smith, F. Hugues, A. Theolier, J. M. Basset, R. Ugo, G. M. Zanderighi, J. L. Bilhou, V. Bilhou-Bougnol and W. F. Graydon, *Inorg. Chem*., 1979, **18**, 3104.
13 R. F. van Slooten and B. E. Nieuwenhuys, *J. Catal*., 1990, **122**, 429.
14 D. Kalakkad, S. L. Anderson, A. D. Logan, J. Pena, E. J. Braunsch-weig, C. H. Peden and A. K. Datye, *J. Phys. Chem*., 1993, **97**, 1437.
15 J. R. Anderson, *Adv. Catal*., 1973, **23**, 1.